Journal of ELECTRONIC MATERIALS, Vol. 42, No. 6, 2013
DOI: 10.1007/s11664-013-2554-7

$Cu_2ZnSnSe_4$ Solar Cells with Absorbers Prepared by the Metallic Ink-Printing Method Using Nanosized Cu-Zn-Sn Pastes and Selenization

DONG-HAU KUO[1,2] and TZUNG-RU JAN[1]

1.—Department of Materials Science and Engineering, National Taiwan University of Science and Technology, Taipei 10607, Taiwan. 2.—e-mail: dhkuo@mail.ntust.edu.tw

A large-grained $Cu_2ZnSnSe_4$ (CZTSe) absorber for solar cells was fabricated by the metallic ink-printing method and subsequent selenization at 600°C to 700°C with overpressures of two different selenium compounds and a step-heating procedure. The developed CZTSe grain size was confirmed as 8 μm to 20 μm. The second heating stage was helpful in inducing crystallization and was important for grain growth. For the nonvacuum approach, nanosized Cu, Zn, and Sn powders were chosen for preparing inks. Ceramic Al_2O_3 was used instead of glass to prevent the thermal decomposition of the substrate. A nanosized $Cu(In,Ga)Se_2$ layer was coated on a Mo electrode to provide a barrier to avoid direct contact of Cu, Zn, and Sn with Mo. The selenization under the combination of two selenide pellets played a crucial role in preparing the CZTSe absorber. The fabricated CZTSe solar cell device showed power conversion efficiency of 1.14%, open-circuit voltage of 130 mV, short-circuit current density of 33.1 mA/cm^2, and fill factor of 0.265.

Key words: $Cu_2ZnSnSe_4$, solar cells, ink printing

INTRODUCTION

Cu_2-II-IV-VI_4 quaternary compounds of $Cu_2ZnSnSe_4$ (CZTSe), Cu_2ZnSnS_4 (CZTS), and their solid solution (CZTSSe) with energy gaps of 1.0 eV to 1.5 eV and absorption coefficients of 10^4 cm^{-1} to 10^5 cm^{-1} are cost-effective materials for thin-film solar cells.[1,2] However, research efforts in Cu_2-II-IV-VI_4, in general, are far behind those in $Cu(In_{1-x}Ga_x)Se_2$.[3,4] Recently, rapid progress in earth-abundant Cu_2-II-IV-VI_4 solar cells with efficiencies of 8% to 10% has indicated that this system has great potential.[2,5–7]

The processes for Cu_2-II-IV-VI_4 solar cells include vacuum and nonvacuum methods. Based upon a vacuum method, Reppins et al.[8] demonstrated 9.15%-efficient cells with absorbers prepared by four-source co-evaporation. Katagiri et al.[9] obtained 6.7%-efficient cells by cosputtering with Cu, SnS, and ZnS targets, followed by sulfurization with H_2S at 580°C. CZTS solar cells with efficiency of 3% to 5% were also fabricated by sequential sputtering deposition of metallic films using multiple targets followed by selenization or sulfurization at high temperatures.[10,11] Using the nonvacuum method, Barkhouse et al.[5] reported high-efficiency (10.1%) CZTSSe cells made using a hydrazine solution and a nonvacuum method followed by an annealing process at 540°C. Redinger et al.[12] reacted an electroplated Cu/Zn stack with decomposed Sn and S(Se) vapors for fabrication of CZTSSe cells with 5.4% efficiency. We also reported enhanced grain growth with $SnSe_2$ to provide the Se vapor for selenization.[13] Other nonvacuum methods did not reach the expected efficiency.[14,15] Basically, the successful hydrazine solution method can leave Cu_2-II-IV-VI_4 films without organic residues, which would prevent good film crystallization. For vacuum- and nonvacuum-based Cu_2-II-IV-VI_4 solar cells, it is important to obtain samples with good crystallization, densification, and

(Received October 23, 2012; accepted February 28, 2013; published online April 4, 2013)

large grain size. Furthermore, the absorption layer needs to be improved in interface reactions, and the porosity for good quality.[16]

Here, we describe a well-crystallized, large-grained CZTSe absorption layer obtained by printing metallic paste of nanosized Cu, Zn, and Sn powders onto CIGSe/Mo-coated alumina substrates followed by selenization at 600°C to 700°C. The selection of nanosized metallic powders is based on their strong reaction activity in order to facilitate densification and grain growth. Soda-lime glass substrate is limited to use below temperature of 600°C. In the present work, alumina substrate was utilized to broaden our processing range above 600°C and to enhance the sintering and grain growth of CZTSe. Because the printing-type powders do not pack densely, a high selenization temperature is needed and control of the composition of CZTSe is quite a challenge. A CIGSe barrier layer is inserted between the Cu-Zn-Sn paste and Mo back electrode to control the interface reactions.

EXPERIMENTAL PROCEDURES

$Cu_2ZnSnSe_4$ thin films formed on CIGSe/Mo-coated alumina (Al_2O_3) substrates were prepared by postselenization of ink-printed Cu-Zn-Sn metallic films at 600°C to 700°C. The Mo back electrode with thickness of 0.8 μm to 1.2 μm was deposited by direct-current (dc) sputtering at 100 W for 2 h. Commercially available nanosized Cu, Zn, and Sn metallic powders with ratio of 0.8:0.55:0.5, respectively, were ball-mixed with an ester-type dispersant to form metallic inks for printing. After ink printing and drying, the dried layers were pressed under uniaxial loading of 100 MPa for 10 min to have a thickness of 8 μm to 12 μm. Postselenization was carried out by a step-heating procedure in a tube furnace. In the first holding stage, the sample was kept at 300°C for 0.5 h, while in the second holding stage it was kept at 600°C, 650°C or 700°C for 1 h. The step-heating procedure is expressed as the 300°C to 700°C two-step procedure, for example. To minimize the interface reactions between metallic Cu, Zn, and Sn and the Mo bottom electrode, a 0.1-μm- to 0.2-μm-thick CIGSe barrier layer was deposited on a Mo-coated alumina substrate by radio frequency (rf) sputtering at 90 W for 0.5 h. The CIGSe target was made by hot pressing the self-synthesized powders. To investigate the film development during the step-heating selenization procedure at 700°C, CZTSe films obtained from selenization of Cu-Zn-Sn films were evaluated at different intermediate stages, as symbolized as stages I to VI in Fig. 1. During the selenization, Cu-Zn-Sn films were loaded in a lid-covered ceramic crucible with a combination of two selenide pellets of $SnSe_2$ and $CuSe_2$. Also $SnSe_2$ and $CuSe_2$ powders were prepared by a powder technique. After selenization, the CZTSe films were deposited on alumina/Mo/CIGSe substrates with dimensions of

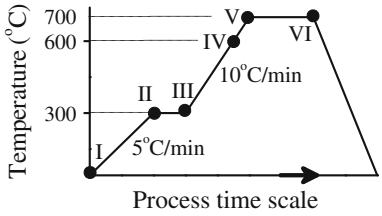

Fig. 1. Different intermediate stages I to VI in the two-step heating profile for Cu-Zn-Sn layers selenized at 700°C for 1 h.

2.5 mm × 4.0 mm. The following procedures were followed to form devices: A 50-nm-thick CdS buffer layer was deposited on the CZTSe absorber layer by chemical bath deposition at 80°C for 15 min in a solution of cadmium acetate, thiourea, ammonium chloride, and ammonia. The 50-nm-thick ZnO and 500-nm-thick indium tin oxide (ITO) layers were individually deposited by radio frequency (rf) sputtering at 200°C for 0.5 h and 1 h, respectively, with home-made targets of ZnO and ITO, both hot-pressed at 1200°C for 30 min. Silver paste was used for electrical contacts. The final cell structure was a stack of the form alumina/Mo/CIGSe/CZTSe/CdS/i-ZnO/ITO/Ag.

The phase composition of CZTSe layers was analyzed by x-ray diffractometry (XRD, Rigaku D/Max-RC). A field-emission scanning electron microscope (SEM, JEOL JSM 6500F) equipped with energy-dispersive x-ray spectroscopy (EDX) was used for microstructural characterization and composition analysis. The illuminated J–V characteristics of the devices were measured using a standard AM1.5 illumination meter.

RESULTS AND DISCUSSION

Metallic ink-printed Cu-Zn-Sn films were selenized by Se-containing vapor provided by simultaneously heating two different pellets of $SnSe_2$ and $CuSe_2$ at high temperature. Figure 2 shows SEM images of metallic ink-printed CZTSe layers after two-step selenization at (a) 600°C, (b) 650°C, and (c) 700°C for 1 h. The CZTSe grain size increased with increasing selenization temperature (T_{Se}). Those selenized below 600°C showed porous microstructure and were not included in this report. However, Cu-Zn-Sn selenized at and above 600°C without a $CuSe_2$ pellet showed severe Cu deficiency as compared with those at 550°C. During selenization, addition of a $CuSe_2$ pellet together with the $SnSe_2$ pellet helped to solve the problem of low Cu content at high T_{Se}. The table inset in Fig. 2 lists the Cu, Zn, Sn, and Se atomic percentages in the CZTSe film after selenization at 600°C, 650°C, and 700°C. The composition analyses of the films selenized at different temperatures showed an average Cu/(Zn + Sn) ratio of 0.82 to 0.96, Zn/Sn ratio of 1.03 to 1.18, and Se/(Cu + Zn + Sn) ratio of 1.02 to 1.06. After selenization at above 600°C, the CZTSe films did not show the problems of constituent element

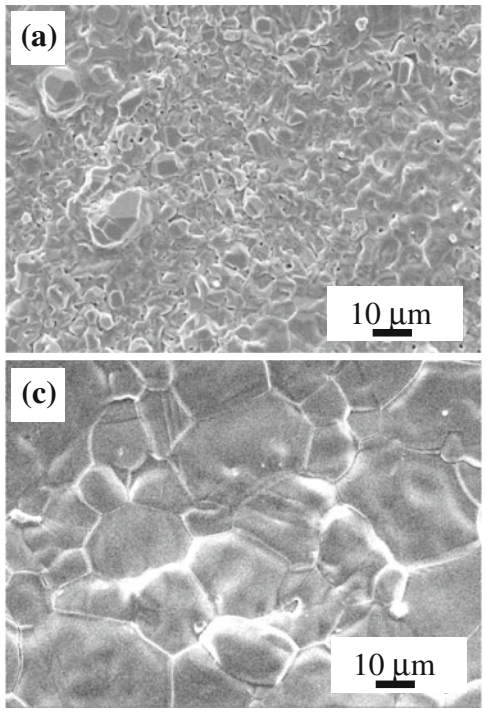

Item	Cu%	Zn%	Sn%	Se%
600°C	21.9 ±1.6	13.5 ±0.7	13.1 ±0.5	51.5 ±1.2
650°C	23.7 ±1.1	13.4 ±0.6	11.4 ±0.4	51.5 ±1.0
700°C	22.7 ±1.3	14.0 ±0.8	12.8 ±0.5	50.5 ±0.8

Fig. 2. SEM images of metallic ink-printed CZTSe layers after two-step selenization at (a) 600°C, (b) 650°C, and (c) 700°C for 1 h. The inset table lists the composition data in atomic percentage for the CZTSe layers after selenization at different temperatures.

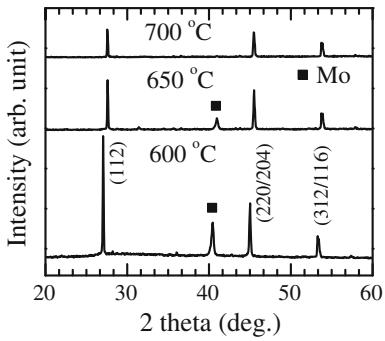

Fig. 3. XRD patterns of metallic ink-printed CZTSe absorption layers after two-step selenization at (a) 600°C, (b) 650°C, and (c) 700°C for 1 h.

deficiency. When the $CuSe_2$ pellet was not used in the selenization, the Cu content was reduced to 17% and the Cu/(Zn + Sn) ratio was less than 0.75.

The 600°C-selenized CZTSe film showed a rough surface and heterogeneous microstructure (Fig. 2a). Dissolution and vaporization of the absorbed Se species interacting with the Cu-Zn-Sn film led to the formation of the poor morphology. During the two-step heating procedure, the first step of holding at 300°C is to provide sufficient Se vapor for the purpose of oversaturation and to form condensed Se liquid on the top of the Cu-Zn-Sn film. When heating to the second step and holding at 600°C, the condensed Se liquid reacts with Cu-Zn-Sn to form volatile vapor species, which leads to the formation of a rough microstructure. The CZTSe films selenized at 650°C and 700°C showed a smooth surface and homogeneous microstructure (Fig. 2b, c). The grain sizes for 650°C- and 700°C-selenized films were 4 μm to 12 μm and 8 μm to 20 μm, respectively. The reason for the different, rough and smooth morphologies could be related to the different degrees of Se or selenide oversaturation at different temperatures, leading to the formation of different copper selenides of Cu_2Se, CuSe, and $CuSe_2$. Stable selenide will aid densification, whereas a volatile one will lead to the formation of a rough microstructure. This finding is based upon the loss of Cu content in our process without a $CuSe_2$ pellet at high T_{Se}. Further investigations on this issue are needed, since it is crucial to control the degree of selenization. The SEM results confirm that selenization with the combination of the two selenide pellets is a correct approach to obtain CZTSe films with characteristic features of dense microstructure without voids, controlled stoichiometry, and large grains.

The CIGSe layer was not observed on cross-sectional imaging after selenization of the CIGSe barrier layer. The In and Ga elements were detected by EDX element point mapping. Once selenization of the Cu-Zn-Sn film begins, a solid solution of CZTSe and CIGSe also formed simultaneously. The effect of In and Ga dissolution into the CZTSe requires further investigation. It is difficult to avoid the reaction between the metal layers of Cu-Zn-Sn and Mo due to the formation of their intermediate compounds,

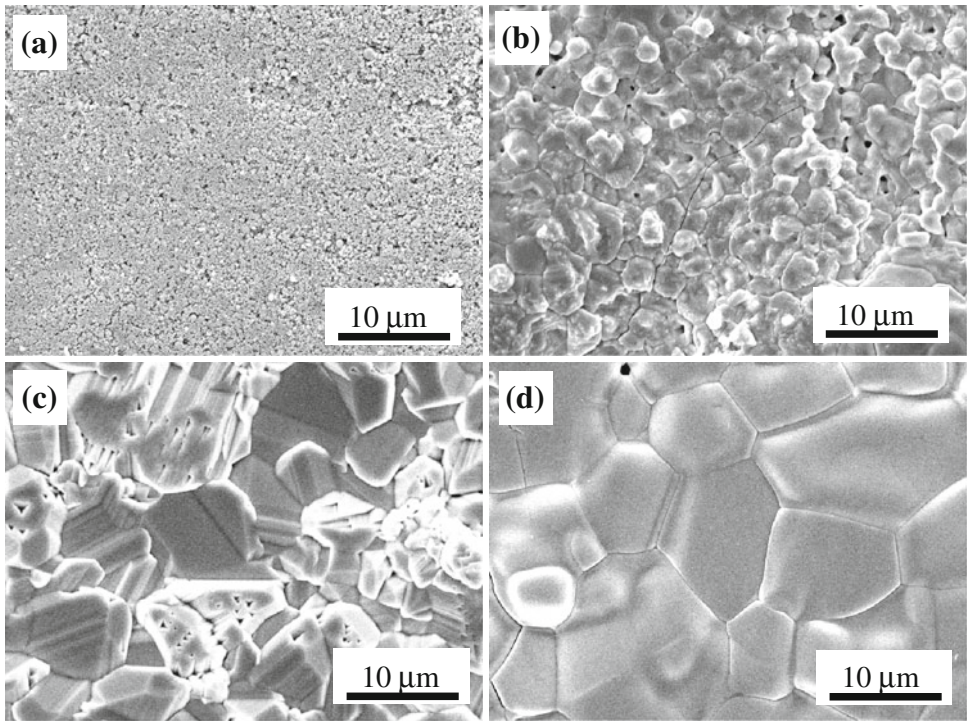

Fig. 4. SEM images of metallic ink-printed CZTSe layers at intermediate heating stages (a) III, (b) IV, (c) V, and (d) VI of a 300°C to 700°C two-step selenization procedure.

based on the Mo-Zn and Mo-Sn binary phase diagrams. Furthermore, as the Cu-Zn-Sn films are selenized, the Mo electrode will also be attacked. The main purpose of the design of the CIGSe layer in the present work is to avoid the predicted interface reactions at high T_{Se} of 600°C to 700°C. A $MoSe_2$ coating could be another candidate barrier layer between Cu-Zn-Sn and Mo, but it is difficult to densify a $MoSe_2$ target for sputtering. Recently, an IBM research team reported 8.9% efficiency for CZTSe solar cells with a TiN diffusion barrier.[17] The diffusion barrier concept has become important.

Figure 3 shows XRD patterns of metallic ink-printed CZTSe absorption layers after two-step selenization at (a) 600°C, (b) 650°C, and (c) 700°C for 1 h. The major diffraction peaks of polycrystalline CZTSe were related to the (112), (220/204), and (312/116) orientations of a kesterite structure.[18] The only second phase came from the contribution of the Mo electrode. There was no $MoSe_2$ phase. The diffraction intensity of Mo decreased with increasing T_{Se}, which is related to an increase in film thickness at high T_{Se}. The grain sizes of the CZTSe films selenized at 600°C, 650°C, and 700°C are 10 μm, 12 μm, and 20 μm, respectively. With the similar paste thickness, this large difference in thickness indicates that there is a strong interaction and reactions between the metallic films and the selenide-contributed Se vapor at higher T_{Se}. However, the diffraction intensity was reduced for the film selenized at 700°C, as shown in Fig. 3c. From the point mapping composition analyses, it was observed that the Mo element had diffused into CZTSe to form a solid solution after selenization at 700°C. Such incorporation of Mo ions leads to lattice distortion and worse crystallinity at higher T_{Se}.

To investigate the microstructural development during the step-heating selenization procedure, metallic ink-printed CZTSe films were heated to intermediate stages. Figure 4 shows SEM images of metallic ink-printed CZTSe layers at intermediate heating stages (a) III, (b) IV, (c) V, and (d) VI using a two-step selenization procedure at 300°C to 700°C. After holding at 300°C for 0.5 h (stage III in Fig. 1), the ink-printed film did not show any grain growth behavior (Fig. 4a). At stage IV, for films heated to 600°C without holding, CZTSe showed nonuniform grains of 1 μm to 4 μm with a rough surface, as shown in Fig. 4b. This is due to dissolution and vaporization of absorbed Se species, which also indicates a weak reaction between the metallic film and Se vapor at 600°C. At stage V, for films heated to 700°C without holding, large grains of 5 μm with trapped voids and stacking defects were observed (Fig. 4c), confirming the fast grain growth process. At stage VI, for films held at 700°C for 1 h, huge CZTSe grains of 8 μm to 20 μm (lower magnification in Fig. 2c, higher magnification in Fig. 4d) were obtained. A very few CZTSe grains larger than 5 μm are seen, especially when using the nonvacuum method. Densification of an ionic compound, e.g., a soda-lime glass powder, is hard to achieve at 500°C to 600°C without any aids. Our experiments aim to selenize CZTSe films at higher temperatures

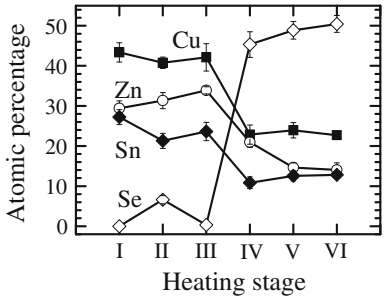

Fig. 5. Composition analyses of metallic ink-printed $Cu_2ZnSnSe_4$ layers at different stages of a 300°C to 700°C two-step selenization procedure using two selenide pellets.

(≥600°C) for the purpose of grain growth. To avoid these confronting problems, we need to use Se-supplying sources for reactive sintering and a CIGSe barrier layer to avoid a strong interface reaction, and to replace the soda-lime glass with an alumina substrate.

Figure 5 shows composition analyses of metallic ink-printed $Cu_2ZnSnSe_4$ layers at different intermediate heating stages at 300°C to 700°C of the two-step selenization procedure. During the step-heating selenization, the Cu-Zn-Sn films showed negligible Se content after holding at 300°C for 0.5 h. As the temperature increased from 300°C to 700°C (stage V), the Cu-Zn-Sn films reacted strongly with Se species to form CZTSe with Se content of 48.9 ± 1.8%. With further 1-h holding at 700°C (stage VI), the selenized films reached Se content of 50.5 ± 1.2%. Our selenization approach helped to induce a strong reaction between the Cu-Zn-Sn metallic films and the Se species at temperatures above 600°C. Due to the effect on the electrical properties, it is desirable to have the correct Se content rather than have Se vacancies as point defects. Fortunately, even when selenized at 700°C, the CZTSe films did not have a Se deficiency problem.

The performance of CZTSe solar cells with the metallic ink-printed absorber selenized at 650°C was investigated. Figure 6a shows a current density–voltage (J–V) plot for the CZTSe solar cell with an illuminated area of 0.1 cm^2. This device showed power conversion efficiency (η) of 1.14%, open-circuit voltage (V_{OC}) of 130 mV, short-circuit current density (J_{SC}) of 33.1 mA/cm^2, and fill factor (FF) of 0.265, under standard AM1.5 illumination. Reported J_{SC} values were smaller than 40 mA/cm^2.[1–8] The lower V_{OC} of 130 mV and fill factor of 0.265 could be improved by lowering the Cu/(Zn + Sn) ratio, obtaining the correct ZnO layer thickness to establish a stable built-in voltage, and replacing Se with S to widen the band gap of CZTSe. CZTSe solar cells with good efficiency have always shown V_{OC} between 380 mV and 640 mV.[2–9] The energy conversion efficiency of the CZTSe cells could be greatly improved by improving the values of V_{OC} and FF.

Figure 6b shows a cross-sectional SEM image of the CZTSe absorption layer after selenization at

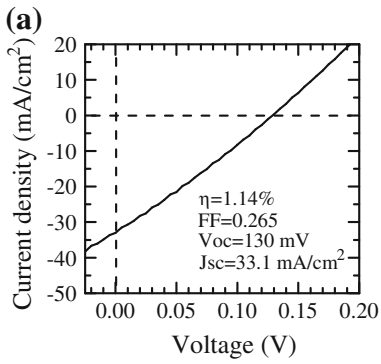

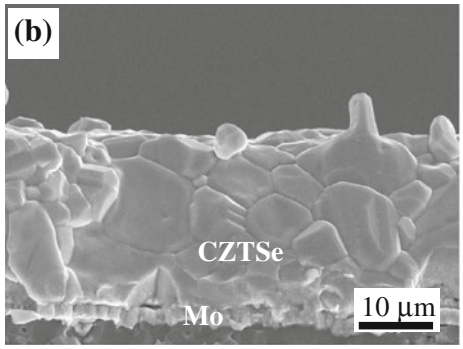

Fig. 6. (a) Current density–voltage (J–V) plot of a CZTSe solar cell. (b) Cross-sectional SEM image of the metallic ink-printed CZTSe absorption layer after selenization at 700°C.

700°C. Limited by the facility, the thickness of the absorption layer was about 20 μm. After selenization, the thickness of the Cu-Zn-Sn film was doubled, i.e., from 8–12 μm to 20 μm, due to the phase transformation from the metallic material to ceramic by selenization. With improvement of our tools, a thin-film solar cell instead of a thick one could be obtained. The thicker CZTSe layer was composed of three to five grains. The trapping of photoinduced electrons and holes by grain boundaries will be minimized. The CZTSe/Mo interface was dense and continuous without porosity. The CIGSe barrier layer in between can contribute to the formation of this good interface. If the metallic films are deposited directly on the Mo electrode, it will be difficult to carry out a selenization process that only selenizes the metallic films without diffusing to and reacting with Mo, which would lead to the formation of a thick $MoSe_2$ layer. Good performance of CZTSe solar cells can be expected when the CZTSe film has large grains and good crystallinity and does not have porosity at the CZTSe/Mo interface. From our work, selenization at 650°C is already good enough to obtain large grain size, good crystallinity, and a dense absorber layer.

Ideal "passivated" grains for the absorption layer of thin-film solar cell devices are grains with film-thick grain size.[19] It is important to have Cu_2-II-IV-VI_4 solar cells with good crystallization, densification, and large grain size of 1 μm to 2 μm.[2,5,6] Conventionally, use of pure Se powder as a vapor

source results in deficiency above 550°C, leading to Se-deficient CZTSe, or porous films due to vaporization at and above 600°C. Herein, we present a procedure to transform simply paste-printed Cu-Zn-Sn metallic films into dense CZTSe films with passivated grains of 8 μm to 20 μm.

CONCLUSIONS

A metallic ink-printed CZTSe absorption layer with large grains of 8 μm to 20 μm was prepared by ink-printing metallic paste of Cu-Zn-Sn followed by selenization at 600°C to 700°C for 1 h in the presence of two selenide pellets. The inks contain nanosized metallic powders that aided densification. During the two-step selenization, the Se content rapidly increased as the temperature increased from 300°C to 600°C. The grain growth process continues during the high-temperature holding. To densify the CZTSe film at high temperature, the $CuSe_2$ pellet helped to solve the problems of (1) Cu loss with selenide pellets, (2) the reactions at the CZTSe/Mo interface with CIGSe, and (3) the heat resistance of substrate with Al_2O_3. These changes in the preparation of CZTSe solar cells by a nonvacuum method further diversify CZTSe processing. Our CZTSe solar cell device showed power conversion efficiency of 1.14%, open-circuit voltage of 130 mV, short-circuit current density of 33.1 mA/cm^2, and fill factor of 0.265.

ACKNOWLEDGEMENTS

This work was supported by the National Science Council of the R.O.C. under Grant Nos. NSC 101-2221-E-011-046 and NSC 101-ET-E-011-001-ET. Dr. K.P.O. Mahesh helped the authors in editing this manuscript.

REFERENCES

1. H. Katagiri, K. Jimbo, W.S. Maw, K. Oishi, M. Yamazaki, H. Araki, and A. Takeuchi, *Thin Solid Films* 517, 2455 (2009).
2. K. Jimbo, R. Kimura, T. Kamimura, S. Yamada, W.S. Maw, H. Araki, K. Oishi, and H. Katagiri, *Thin Solid Films* 515, 5997 (2007).
3. T.M. Razykov, C.S. Ferekides, D. Morel, E. Stefanakos, H.S. Ullal, and H.M. Upadhyaya, *Sol. Energy* 85, 1580 (2011).
4. C.J. Hibberd, E. Chassaing, W. Liu, D.B. Mitzi, D. Lincot, and A.N. Tiwari, *Prog Photovolt.: Res. Appl.* 18, 434 (2010).
5. D. Aaron, R. Barkhouse, O. Gunawan, T. Gokmen, T.K. Todorov, and D.B. Mitzi, *Prog. Photovolt.: Res. Appl.* 20, 6 (2012).
6. T.K. Todorov, K.B. Reuter, and D.B. Mitzi, *Adv. Mater.* 22, E156 (2010).
7. S. Bag, O. Gunawan, T. Gokmen, Y. Zhu, T.K. Todorov, and D.B. Mitzi, *Energy Environ. Sci.* 5, 7060 (2012).
8. I. Repins, C. Beall, N. Vora, C. DeHart, D. Kuciauskas, P. Dippo, B. To, J. Mann, W.C. Hsu, A. Goodrich, and R. Noufi, *Sol. Energy Mater. Sol. Cells* 101, 154 (2012).
9. H. Katagiri, K. Jimbo, S. Yamada, T. Kamimura, W.S. Maw, T. Fukano, T. Ito, and T. Motohiro, *Appl. Phys. Express* 1, 041201 (2008).
10. G. Zoppi, I. Forbes, R.W. Miles, P.J. Dale, J.J. Scragg, and L.M. Peter, *Prog Photovolt.: Res. Appl.* 17, 315 (2009).
11. R.B.V. Chalapathy, G.S. Jung, and B.T. Ahn, *Sol. Energy Mater. Sol. Cells* 95, 3216 (2011).
12. A. Redinger, D.M. Berg, P.J. Dale, and S. Siebentritt, *J. Am. Chem. Soc.* 133, 3320 (2011).
13. D.H. Kuo, W.D. Haung, Y.S. Huang, J.D. Wu, and Y.J. Lin, *Surf. Coat. Technol.* 205, S196 (2010).
14. K. Tanaka, Y. Fukui, N. Moritake, and H. Uchiki, *Sol. Energy Mater. Sol. Cells* 95, 838 (2011).
15. H. Araki, Y. Kubo, K. Jimbo, W.S. Maw, H. Katagiri, M. Yamazaki, K. Oishi, and A. Takeuchi, *Phys. Status Solidi C* 6, 1266 (2009).
16. K. Wang, B. Shin, K.B. Reuter, T. Todorov, D.B. Mitzi, and S. Guha, *Appl. Phys. Lett.* 98, 051912 (2011).
17. B. Shin, Y. Zhu, N.A. Bojarczuk, S.J. Chey, and S. Guha, *Appl. Phys. Lett.* 101, 053903 (2012).
18. S. Schorr, *Sol. Energy Mater. Sol. Cells* 95, 1482 (2011).
19. J.R. Sites, J.E. Granata, and J.F. Hiltner, *Sol. Energy Mater. Sol. Cells* 55, 43 (1998).